

# Cross-polarization As a Function Of Frequency For An Axisymmetric Paraboloidal Reflector

Y. Thakore\* and S.W. Ellingson

June 22, 2024

## 1 Introduction

An array of Paraboloidal axisymmetric is a general setting used in Radio Astronomy to study the space activities. These arrays are designed for a specific center frequency. However, it cannot be the ideal condition always and so, the system should be functioning even when the frequency is shifted. When the Electronically Reconfigurable Surface (ERS) is implemented to cancel the interference in a specific direction, we also notice a little change in the cross-pol pattern. This report is a case study of the behaviour of cross-pol of 18 meter diameter axisymmetric paraboloidal reflector designed for a center frequency of 1.5 GHz, which is shifted from 1.4 GHz to 1.6 GHz.

## 2 Cross-Polarization and Co-Polarization

The magnitude of the radiation pattern polarized in the desired direction is called Co-Polarization. Whereas, the magnitude of the radiation pattern polarized in the direction other than the intended direction is called as Cross-Polarization. For 18m diameter paraboloidal axisymmetric reflector, the feed is assumed to be Huygen's source. A Huygen's source feed contains electrically short electric and magnetic dipole perpendicular to each other. One of the main advantage of a Huygen's source feed is low cross-polarization level. The feed can be modelled as

$$E_i = E_0(\hat{y}_f \times \hat{r}_f \times \hat{r}_h + \hat{x}_f \times \hat{r}_f) \frac{e^{-j\beta r_f}}{r_f}$$

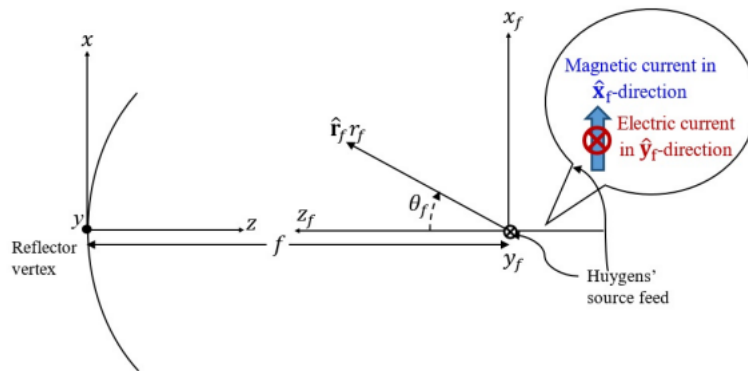


Fig. 1. Co-ordinate system of the feed (Image credit: [1])

---

\*Bradley Dept. of Electrical and Computer Engineering, Virginia Tech. e-mail: yugma@vt.edu

From the geometry of the figure,  $\hat{y}$  is the desired direction of radiation and so will be the co-polarization vector. A generalized form of the polarization vector in the form of spherical coordinates can be found from [2]

$$e_{co}^{\hat{}} = \sin\phi_p \hat{\theta} + \cos\phi_p \hat{\phi}$$

$$e_{cr}^{\hat{}} = \cos\phi_p \hat{\theta} - \sin\phi_p \hat{\phi}$$

The  $\phi_p$  is the plane angle of observation which in our case is H-plane ( $\phi = 0^\circ$ ). For an 18m diameter dish having f/D ratio=0.4, the angle from the z axis to the edge of the dish can be calculated by

$$\theta_0 = 2\arctan\left(\frac{1}{4f/D}\right) = 64.01^\circ$$

### 3 Directivity

The directivity of the system can be determined by using physical optics approximation. According to the physical optics approximation, the reflecting surface can be considered to be electrically large and perfectly conducting surface whose surface current distribution can be given by

$$J_s = 2\hat{n} \times H^i$$

where

$$H^i(s^i) = I_0 \frac{\hat{y} \times \hat{s}^i}{|\hat{y} \times \hat{s}^i|} \frac{e^{-jks^i}}{s^i} (\cos\theta_f)^q$$

$\hat{s}^i$  is a unit vector pointing from the center of the aperture dish to the observation point and  $\hat{n}$  is the unit vector normal to the point on the reflector. Here, q=1.14, which results in the aperture efficiency of 81.5% and an edge illumination of approximately -11 dB. The scattered electric field will be

$$E^s = -\frac{j\omega\mu_0}{4\pi r} e^{-j\beta r} \int_{\theta_f=0}^{\theta_f} \int_{\phi=0}^{2\pi} J_s e^{j\beta \hat{r} \cdot \mathbf{r}'} ds$$

The differential surface  $ds = \frac{\sqrt{4f^2 + \rho^2}}{2f}$  is obtained by gridding the surface of the reflector into small patches. The angle from the feed to the point on the reflector under evaluation is given by  $\theta_f$ .

Directivity can be defined as the ratio of the maximum power density and the power density averaged over all directions.

$$G(\hat{r}) = \frac{S(r\hat{r})}{< S(r\hat{r}) >}$$

$$S(r\hat{r}) = \frac{|E^s(r\hat{r})|^2}{2\eta_0}$$

The average power density can be calculated by determining the radiated power first.

$$P_{rad} = \int_{\theta=0}^{\pi} \int_{\phi=0}^{2\pi} S(R\hat{r}) R^2 \sin\theta d\theta d\phi$$

And so,

$$< S(R\hat{r}) > = \frac{P_{rad}}{4\pi R^2} = \frac{1}{4\pi} \int_{\theta=0}^{\pi} \int_{\phi=0}^{2\pi} S(R\hat{r}) \sin\theta d\theta d\phi$$

The pattern can thus be given by,

$$\tilde{\phi}(\hat{r}) = \hat{e} \cdot E^s(\hat{r})$$

$\hat{e}$  can be replaced with  $e_{co}^{\hat{}}$  or  $e_{cr}^{\hat{}}$ , whichever is required.

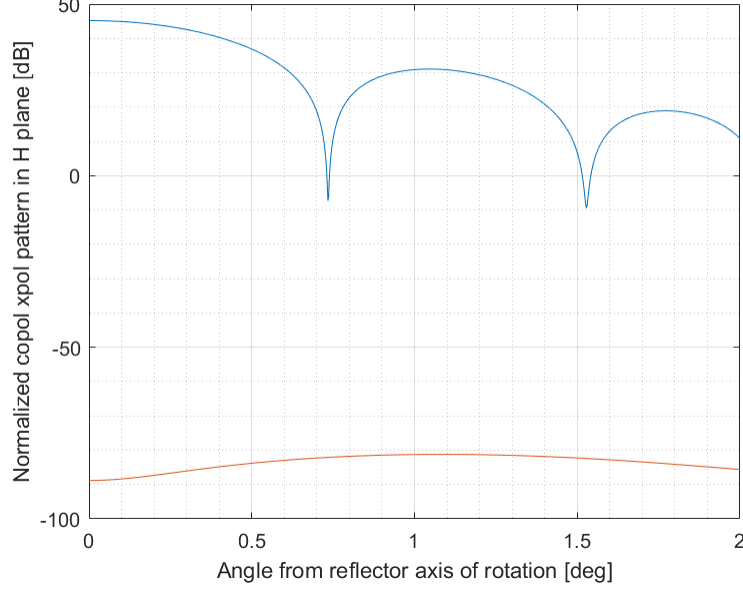


Fig. 2. Co-polarization(red) and cross polarization(blue) component in H-Plane

Figure shows the solid blue line as the co-pol pattern and the solid red line as the cross-pol pattern in H-Plane according to the system assumptions we made previously.

## 4 Implementation of ERS

One of the most common issue these array of ground reflectors are facing is the interference by LEO satellites. The radiation pattern can be affected by the interference through sidelobes which can be modified by considering the rim of the reflector as unit cells whose phase of scattering can be controlled. These unit cells of subwavelength dimension are assumed to be contiguous.

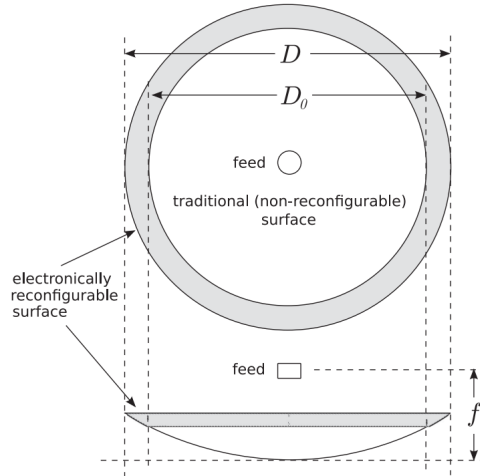


Fig. 3. On-axis(top) and side(bottom) views of an electronically reconfigurable rim scattering system (Image Credit: [2])

For the 18m axisymmetric circular prime-fed paraboloidal dish, we are considering the width of the rim to be 0.5m, leaving the diameter of the dish to be 17m. The logic behind keeping the new diameter to be as less by just 1m is that the main lobe of the pattern should not be affected when modifying

the side lobe. The 0.5m rim consists of 2756 contiguous half-wavelength-square flat plates instead of the continuous surface.

## 5 Phase Manipulation of ERS

Reconfigurable surfaces can be controlled by changing their phase. Each unit cells are assigned when practically implementing, we may need to limit the phase to discrete values. The scattered electric field is now calculated by

$$E_1^s = -j\omega\mu_0 \frac{e^{-jkr}}{4\pi r} \sum_n J_1(s_n^i) e^{jk\hat{r} \cdot s_n^i} \Delta s$$

which is the same as calculating the scattered electric field at a point on the reflector except that the integrand is now limited to the dimensions of the plate i.e.  $\Delta s = 0.25\lambda^2$ . Here,  $n$  is used to index the individual cell or plate. Thus, the total scattered electric field will be  $E^s = E_0^s + E_1^s$ . Moreover,

$$J_1(s_n^i) = c_n J_0(s_n^i)$$

where  $c_n$  is a complex constant whose value is assigned to each plate according to the degree of reconfigurability.

$$c_n = \exp\{-j \arg[J_0(s_n^i) e^{jk\hat{r} \cdot s_n^i}]\}$$

In the quiescent state, the value of  $c_n = 1$  for all cells, making the reconfigurable surface a continuous part of the reflector. 1 bit phase quantization limits the value of  $c_n$  to  $\pm 1$  whereas 2 bit phase quantization yields the values of  $c_n$  to be  $+1, +j, -1$  or  $-j$ . The algorithm to decide the value of  $c_n$  for each unit cell is designed in a way that reduces the magnitude of the pattern in the quiescent state.

### 5.1 Serial Search Algorithm

For 1 bit phase quantization, the value of  $c_n$  is either  $+1$  or  $-1$ , depending on whichever value will reduce the total scattered electric field at that step of the integration. Consider  $E_0^s$  to be the value of the scattered electric field for a reflector system with diameter  $D_0 = 17m$ . Now, since the side lobe peaks at  $1.75^\circ$  in the quiescent state of the system, the serial search algorithm picks the set of values of  $c_n$  ( $\pm 1$ ) of the cells which reduces the current magnitude of the scattered electric field during the evaluation. This algorithm yields a deep null at  $1.75^\circ$  resulting into the cancellation of the side lobe created when the system is in quiescent state.

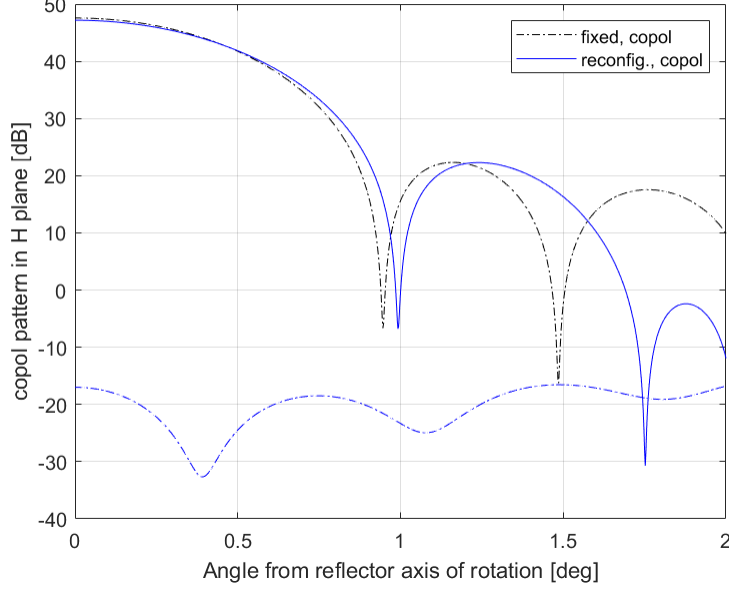


Fig. 4. Deep null obtained at  $\theta = 1.75^\circ$  along with the co-polarization magnitude(solid blue) and cross polarization magnitude(dotted blue) when implemented 1 bit phase quantization

The dotted blue line represents the cross polarization component of the electric field. But, this reading is at the center frequency of 1.5 GHz. However, it is not necessary for the system to always function at a specific center frequency. It should be capable of operating even when shifted from the designated center frequency in order to improve sustainability. Let us take a look at the behaviour of cross-pol component when the center frequency ranges from 1.4 GHz to 1.6 GHz. It is important to note that the state of the system remains unchanged. Thus, the set of values of  $cn_s$  will be the same as it would be for the case of nulling at  $1.75^\circ$  at 1.5 GHz.

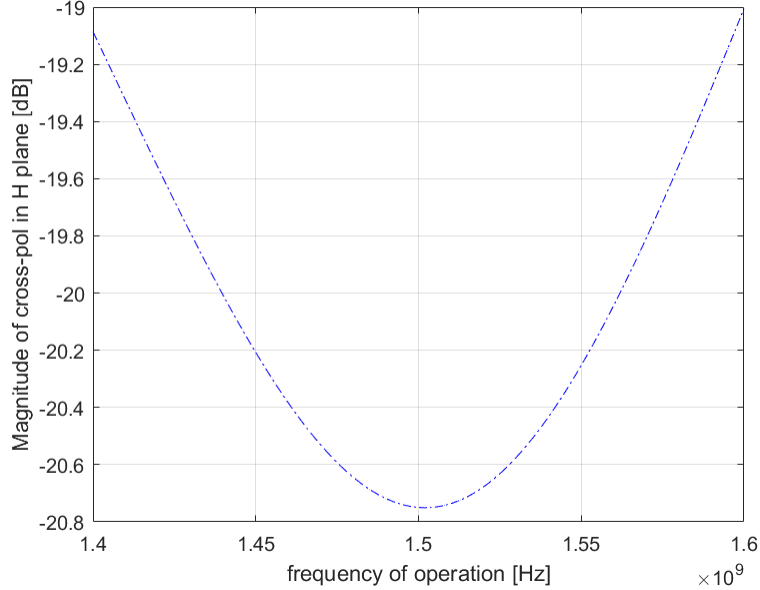


Fig. 5. Magnitude of cross polarization component in H-Plane as a function of frequency when nulling is implemented at  $\theta = 1.75^\circ$

The magnitude of the cross-pol in H-Plane is minimum at 1.5 GHz which is not a surprise since the system is designed keeping in mind 1.5 GHz as the center frequency.

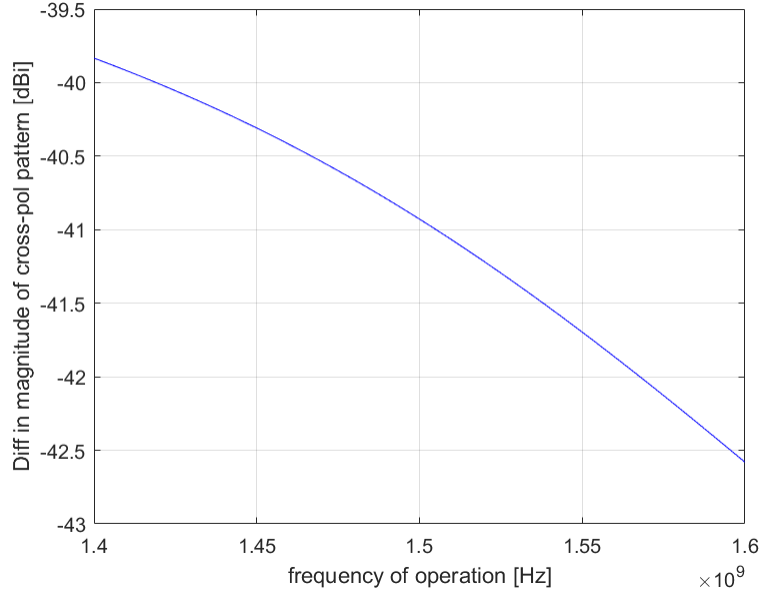


Fig. 6. Difference in the magnitude of the cross polarization component as a function of frequency when ERS with 1 bit phase quantization and the magnitude of the cross polarization component in quiescent state

The difference is observed greatest at 1.4 GHZ and experiences a gradual decline as the frequency of operation increases.

## 6 References

- [1] Ramonika Sengupta and Steven Ellingson, "Adaptive Pattern Modeling for Large Reflector Antennas", *Virginia Tech*, July 2022
- [2] Steven Ellingson and Ramonika Sengupta, "Sidelobe Modification for Reflector Antennas by Electronically Reconfigurable Rim Scattering," *IEEE Trans. Antennas Propag.*, vol.20,no. 6, pp. 1, June 2021